

Bone histology of *Azendohsaurus laaroussii*: Implications for the evolution of thermometabolism in Archosauromorpha

Jorge Cubo and Nour-Eddine Jalil

Abstract.—This paper is aimed at constraining the phylogenetic frame of the acquisition of endothermy by Archosauromorpha. We analyzed the bone histology of *Azendohsaurus laaroussii*. Stylopodial and zeugopodial bones show three tissue types: (1) avascular lamellar zonal bone formed at low growth rates; (2) a scaffold of parallel-fibered bone containing either small primary osteons or simple vascular canals; and (3) fibrolamellar bone formed at high growth rates. We used quantitative histology to infer the thermometabolic regime of this taxon. We define endothermy as the presence of any mechanism of nonshivering thermogenesis that increases both body temperature and resting metabolic rate. Thus, estimating the resting metabolic rate of an extinct organism may be a good proxy to infer its thermometabolic regime (endothermy vs. ectothermy). High resting metabolic rates have been shown to be primitive for the clade *Prolacerta*–Archosauriformes. Therefore, we inferred the resting metabolic rates of *A. laaroussii*, a sister group of this clade, and of 14 extinct related taxa, using phylogenetic eigenvector maps. All the inferences obtained are included in the range of variation of resting metabolic rates measured in mammals and birds, so we can reasonably assume that all these taxa (including *Azendohsaurus*) were endotherms. A parsimony optimization of the presence of endothermy on a phylogenetic tree of tetrapods shows that this derived character state was acquired by the last common ancestor of the clade *Azendohsaurus*–Archosauriformes and that there is a reversion in Crocodylia.

Jorge Cubo. Sorbonne Université, Muséum national d'Histoire naturelle, CNRS, Centre de Recherche en Paléontologie–Paris (CR2P), 4 place Jussieu, BC 104, 75005 Paris, France. E-mail: jorge.cubo_garcia@sorbonne-universite.fr

Nour-Eddine Jalil. Muséum national d'Histoire naturelle, Sorbonne Université, CNRS, Centre de Recherche en Paléontologie–Paris (CR2P), 75005 Paris, France; and Laboratory of Biodiversity and Dynamic of Ecosystems, Department of Geology, Faculty of Sciences Semlalia, University Cadi Ayyad, Marrakesh, Morocco. E-mail: nour-eddine.jalil@mnhn.fr

Accepted: 27 March 2019

Data available from the Dryad Digital Repository: <https://doi.org/10.5061/dryad.qc86g11>

Introduction

The bone histology of non-archosaurian archosauromorphs has received great attention in the last decade (Ricqlès et al. 2008; Nesbitt et al. 2009; Botha-Brink and Smith 2011; Werning and Irmis 2011; Legendre et al. 2013, 2016; Ezcurra et al. 2014; Mukherjee 2015; Veiga et al. 2015; Werning and Nesbitt 2016; Jaquier and Scheyer 2017). Ricqlès et al. (2008) suggested that the capacity of reaching and maintaining very high bone growth rates is an apomorphic feature of archosauriforms. Botha-Brink and Smith (2011) showed that this capacity may have been acquired in a more inclusive node, by the last common ancestor of the clade *Prolacerta*–archosauriforms, with a reversion in *Vancleavea* (see also Nesbitt et al. 2009). Padian and Horner (2002) hypothesized that “the types of tissue deposited in the bones of extinct animals are the most direct evidence

of basal metabolic rates, because they directly reflect growth rates [...]. The sustained deposition of fast-growing bone tissues, as displayed by mammals, birds and other dinosaurs, must reflect sustained high basal metabolic rates” (p. 123). Montes et al. (2007) provided evidence for this hypothesis by showing that the variation of bone growth rates significantly explains the variation of resting metabolic rates in a sample of extant amniotes. They argued that this is due to the fact that high rates of protein synthesis and degradation involved in the periosteal osteogenesis and endosteal osteolysis are energy consuming (Montes et al. 2007). Consistently, Legendre et al. (2016) inferred resting metabolic rates of a sample of Archosauromorpha using quantitative bone histology and phylogenetic eigenvector maps. Interestingly, they inferred a resting metabolic rate of

Prolacerta included within the range of variation of extant mammals (Legendre et al. 2016). Resting metabolic rate depends on bone growth rate (as noted earlier), but it depends also on the presence of thermogenetic mechanisms. We define endothermy as the presence of any mechanism of nonshivering thermogenesis (e.g., Lowell and Spiegelman 2000; Rowland et al. 2015; Nowack et al. 2017) that increases both body temperature and resting metabolic rate. Thus, the resting metabolic rate of an extinct organism may be a good proxy to infer its thermometabolic regime (endothermy vs. ectothermy). Using this proxy, the results obtained by Legendre et al. (2016) suggest that endothermy may have been acquired by the last common ancestor of the clade *Prolacerta*–archosauriforms. The next step to better constrain the phylogenetic frame of the acquisition of endothermy by Archosauromorpha involves inferring the resting metabolic rate of Allokotosauria, the sister-group of the clade *Prolacerta*–archosauriforms (Nesbitt et al. 2015; see also Ezcurra 2016). Therefore, we analyzed the bone histology and inferred the resting metabolic rates of *Azendohsaurus laaroussii* (Archosauromorpha: Allokotosauria; Nesbitt et al. 2015; Ezcurra 2016) using phylogenetic eigenvector maps.

Materials and Methods

Materials

We histologically analyzed skeletal remains from the non-archosauriform archosauromorph *A. laaroussii* from the Upper Triassic (Carnian) of the Argana Basin (Morocco) deposited at the Muséum National d'Histoire Naturelle (MNHN). *Azendohsaurus laaroussii* Dutuit, 1972 was originally described on the basis of a dental fragment and two isolated teeth specialized for plant feeding (Dutuit 1972). On the basis on comparison with ornithischian dinosaurs such as *Fabrosaurus* and *Scelidosaurus*, it was attributed to a new ornithischian dinosaur, making it one of the earliest dinosaurs to be identified (Dutuit 1972; Thulborn 1973, 1974; Bonaparte 1976; Galton 1985, 1990; Weishampel 1990; Gauffre 1993; Hunt and Lucas 1994; Flynn et al. 1999). In addition to the craniodental remains, hundreds of disarticulated and monospecific postcranial remains have been recovered from the *locus typicus* of *A.*

laaroussii (Dutuit 1976). The analysis of these specimens argues strongly against a phylogenetic position inside Dinosauria (Jalil and Knoll 2002). Flynn et al. (2010) named the new species *Azendohsaurus madagaskarensis* from the Triassic of Madagascar and provided for the first time a comprehensive description of the cranial anatomy of the genus. More recently, Nesbitt et al. (2015) provided an extensive description the postcranial anatomy of *A. madagaskarensis*, which is now one of the best-known early archosauromorphs.

All the available postcranial material in the MNHN collection attributed to *A. laaroussii* is monotypic (Khaldoun 2014). It was collected from the *locus typicus* of *A. laaroussii* during the same initial field season (Dutuit 1976) and strongly resembles the postcranial skeleton of *A. madagaskarensis* (Fig. 1). This material can be confidently attributed to *A. laaroussii*. Among the diagnostic postcranial characters of the Malagasy form, only two can be checked on the available material of *A. laaroussii*, and both are present: a posteriorly expanded T-shaped interclavicle and hyposphene-hypantra intervertebral articulations in anterior trunk vertebrae. This later character state was considered autapomorphic for *A. madagaskarensis* by Nesbitt et al. (2015), but it may be a synapomorphy for the genus *Azendohsaurus*. The proportions of the studied skeletal elements MNHN.F.ALM 435 (right humerus), MNHN.F.ALM 497 (left femur), and MNHN.F.ALM 369 (right tibia) show that they are from different specimens.

Histological Methods

Skeletal elements were molded and cast before sectioning to preserve morphological information. Casts and bone remains after histological sampling were repositated at the paleontology collection of the MNHN, where they are available upon a request to the curator. Mid-diaphyses were embedded in epoxy resin and processed histologically following standard procedures (Lamm 2013). Transverse sections as well as longitudinal sections (at the anterior, posterior, dorsal, and ventral sides for humerus and femur and at the anterior, posterior, medial, and lateral sides for the tibia) were obtained and mounted on glass slides. These were analyzed and photographed in a

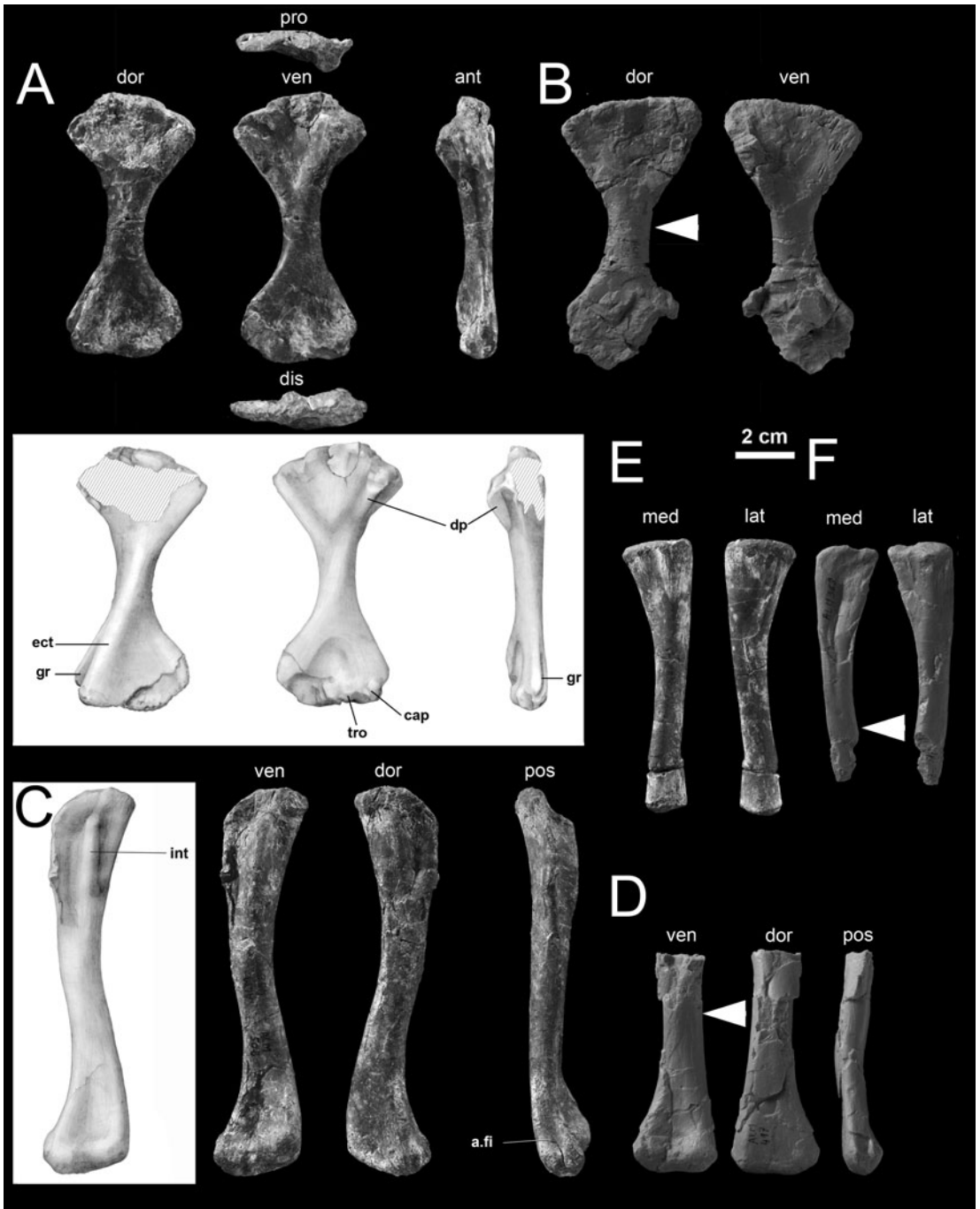


FIGURE 1. *Azendohsaurus laaroussii* Dutuit, 1972 (Argana Basin, Irohalène Member, Carnian): A, B, MNHN.F.ALM 586 left humerus (A) and mold of MNHN.F.ALM 435 right humerus (B) in dorsal (dor), ventral (ven), anterior (ant), proximal (pro), and distal (dis) views; C, D, MNHN.F. ALM 498 and 502, two ends of the same left femur glued (C) and mold of MNHN.F.ALM 497 left femur (D) in ventral, dorsal, and posterior (pos) views; E, F, MNHN.F.ALM 398 right tibia (E) and MNHN.F.ALM 369 mold of right tibia (F) in medial (med) and lateral (lat) views. The arrowheads show the level of the thin sections. Other abbreviations: a.fi, articulation for fibula; cap, capitellum; dp, deltopectoral crest; ect, ectepicondyle; gr, groove; int, internal trochanter; tro, trochlea.

Nikon Eclipse E600POL microscope using normal light and cross-polarized light with a lambda compensator. Thin sections were repositied at the vertebrate hard tissues histological collection of the MNHN, where they are available upon request to the curator (thin sections MNHN-F-HISTOS 2348 to 2362).

Qualitative Histology

The nomenclature and classification of bone tissues is based on bone organization at different integration levels (Francillon-Vieillot et al. 1990). At the level of bone matrix organization, three character states have been defined based on the organization of collagen fibers: the presence (or absence) of woven-fibered bone matrix (WB), parallel-fibered bone matrix (PFB), and lamellar bone matrix (LB). At the level of organization of bone as a tissue, two character states have been defined based on the organization of the collagen fibers, the vascular density, and the cyclicity of bone apposition: the presence of lamellar-zonal bone (LZB) and the presence of the fibrolamellar bone (FLB). See Francillon-Vieillot et al. (1990) for a detailed description of these character states. This pattern-oriented approach has been recently expanded toward a process-oriented view based on the developmental origin of the components of bone tissue (Prondvai et al. 2014). In process-oriented paleohistology, the developmental mechanisms involved in the formation of bone tissue are inferred from the fine architecture of the bone matrix. PFB and LB are formed by the process of dynamic osteogenesis, whereas WB is formed by the process of static osteogenesis (Ferretti et al. 2002; Palumbo et al. 2004; Marotti 2010; Prondvai et al. 2014; Stein and Prondvai 2014; Cubo et al. 2017). Cortices can also have a composite nature, including (1) a scaffold of WB formed by the process of static osteogenesis and (2) centripetal layers infilling primary osteons made of PFB or LB formed by the process of dynamic osteogenesis. This last tissue type has been named “woven-parallel complex” by Prondvai et al. (2014). In the context of process-oriented paleohistology, the widely used term “FLB” is a special case of a woven-parallel complex in which there is abundant woven bone and dense vascularity in the form of primary osteons (Prondvai et al. 2014).

Quantitative Histology

We quantified the vascular density (number of vascular canals by square millimeter) in four orthogonal transects of the transverse sections of humerus, femur, and tibia of *A. laaroussii*. We used the data set published by Legendre et al. (2016) for comparative purposes. It contains the resting metabolic rates and the vascular densities of humerus, femur, and tibia of a sample of 13 extant species and 14 extinct species of tetrapods. Data for *Mus musculus* were removed, because this species was an outlier.

Phylogenetic Comparative Methods

We tested whether vascular density explains a significant fraction of the variation of resting metabolic rate using phylogenetic generalized least-squares regressions (PGLS; Grafen 1989), with the ‘caper’ package (Orme et al. 2013) in R (R Core Team 2016). For this, we used the data set and the phylogeny published by Legendre et al. (2016).

Moreover, we inferred the resting metabolic rates of *A. laaroussii* and those for 14 species of extinct tetrapods using phylogenetic eigenvector maps (Guenard et al. 2013) with the ‘MPSEM’ package (Guenard et al. 2013) in R (R Core Team 2016). For this, we used our data from *A. laaroussii* and the data set and the phylogeny published by Legendre et al. (2016).

Finally, we performed an optimization of the presence of fibrolamellar bone (using our data for *A. laaroussii* and published data for other Archosauromorpha) and an optimization of the presence of endothermy (using observed resting metabolic rates for extant species and inferred resting metabolic rates for extinct ones as a proxy for the thermometabolic regime) onto phylogenies of Archosauromorpha and Tetrapoda, respectively, using parsimony in Mesquite (Maddison and Maddison 2015).

Results

Bone Histology of *Azendohsaurus laaroussii*

Supplementary Fig. 1 shows composite images of the entire diaphyseal cross sections of humerus, femur, and tibia. The medial region of the transverse section of the tibia is avascular (Fig. 2A). The bone matrix appears

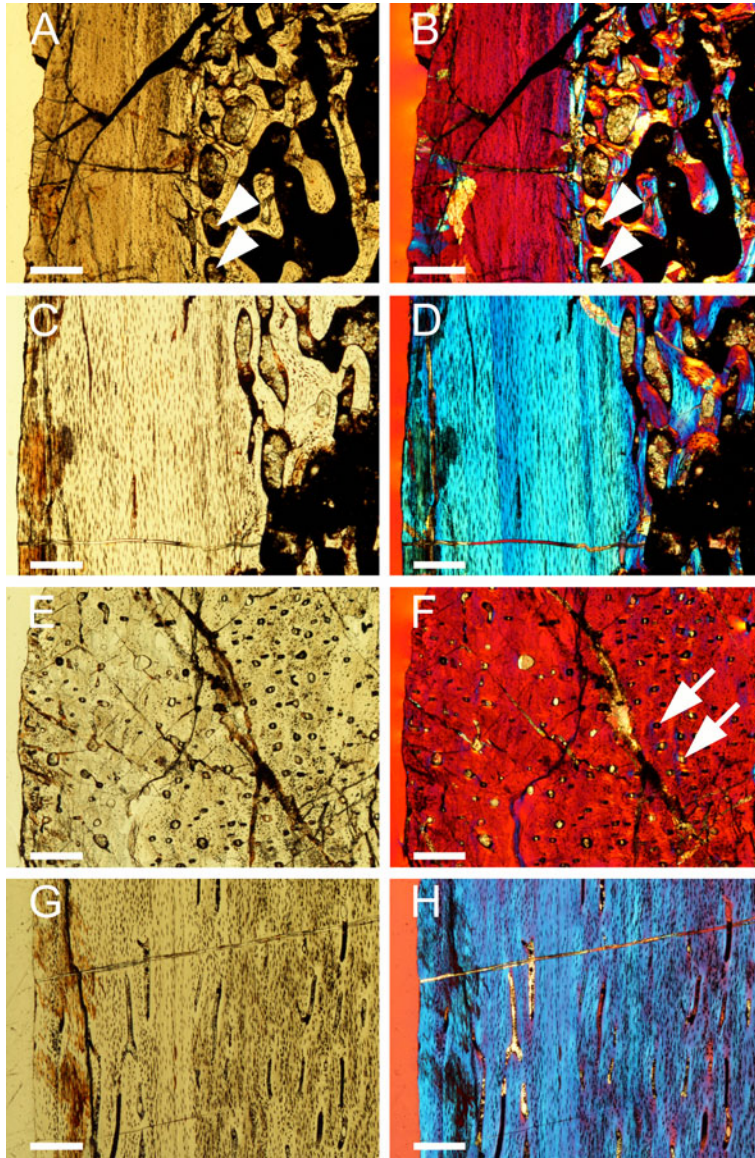


FIGURE 2. Transverse (A, B, E, F) and longitudinal (C, D, G, H) sections of the medial (A–D) and posterior (E–H) regions of the right tibia MNHN.F.ALM 369 of *Azendohsaurus laaroussii* under normal light (A, C, E, G) and cross-polarized light with lambda compensator (B, D, F, H). Periosteum is on the left. Arrows, primary osteons; arrowheads, erosion cavities lined along its periphery by a coating of endosteal lamellar tissue. Scale bars, 300 μm .

isotropic (red in online figure) under cross-polarized light with a lambda compensator (Fig. 2B) and black in cross-polarized light without a lambda compensator (not shown). This can be interpreted either as woven bone or as parallel-fibered bone with fibers perpendicular to the transverse plane of section (Stein and Prondvai 2014). The longitudinal section of the same (medial) region is also

avascular (Fig. 2C). In the longitudinal section, the bone matrix appears anisotropic (blue in online figure, but it can be yellow depending on the orientation to the polarizers) under cross-polarized light with a lambda compensator (Fig. 2D). These complementary patterns of interference suggest that the cortex is composed of parallel-fibered bone, with collagen fibers running parallel to the longitudinal axis

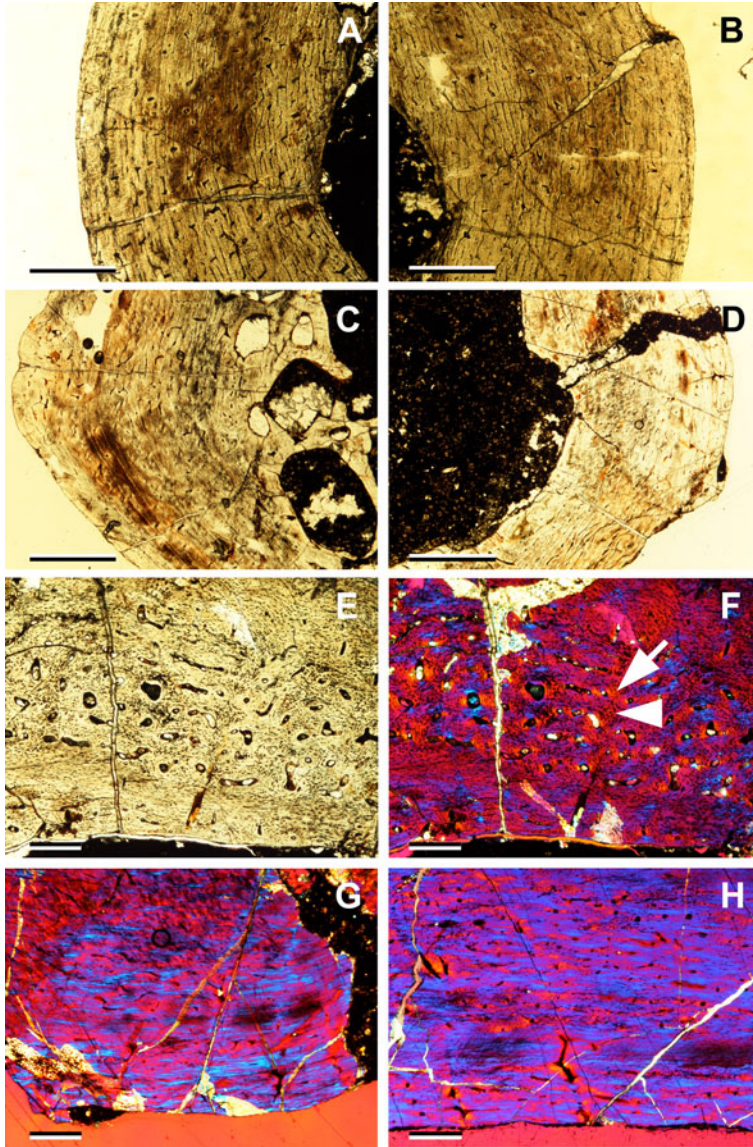


FIGURE 3. Transverse sections of the left femur MNHN.F.ALM 497 (A, anterior region; B, posterior region; E, F, postero-dorsal region) and the right humerus MNHN.F.ALM 435 (C, anterior region; D, posterior region; G, posterior region with higher magnification) and a longitudinal section of the same humerus (H, posterior region) of *Azendohsaurus laaroussii* under normal light (A–E) and cross-polarized light with lambda compensator (F–H). Periosteum is on the left in A and C, on the right in B and D, and at the bottom in G. Endosteum is at the bottom in E, F, H. Arrow, primary osteon; arrowhead, woven bone. Scale bars, 1 mm (A–D); 300 μ m (E–H).

of the tibia. Osteocyte lacunae have a rounded aspect in the transverse section (Fig. 2A,B) and an elongate spindle shape in the longitudinal section (Fig. 2C,D). Their main axis is thus aligned with the collagen fibers of the surrounding matrix, whereas the canaliculi are perpendicular (Fig. 2C,D). We can observe erosion cavities lined by a coating of endosteal

lamellar tissue around the medullary cavity (Fig. 2A,B).

The posterior region of the transverse section of the tibia is well vascularized (Fig. 2E). Vascular density is higher in the deep cortex than in the outer cortex. Vascular canals are longitudinal: they are rounded in transverse section (Fig. 2E,F) and elongated (with the main axis

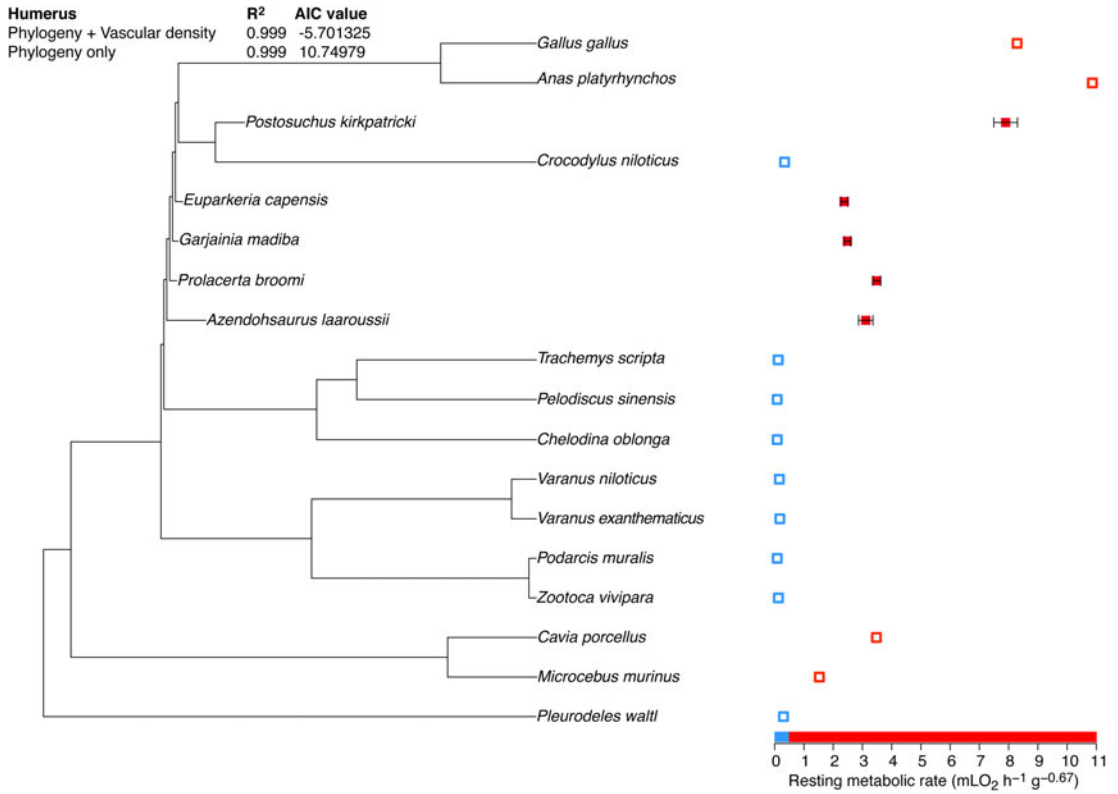


FIGURE 4. Resting metabolic rates quantified in a sample of extant tetrapods and inferred in a sample of extinct Archosaur-omopha using the phylogeny and the vascular density of the humerus. Data for *Azendohsaurus laaroussii* were obtained in this study and data for other taxa as well as the phylogeny were taken from Legendre et al. (2016). Resting metabolic rates inferred for *Azendohsaurus*, *Prolacerta*, *Garjainia*, and *Euparkeria* are in the range of variation of extant mammals, whereas the value inferred for *Postosuchus* is in the range of variation of extant birds.

parallel to the main axis of the tibia) in the longitudinal section (Fig. 2G,H). The scarce vascular canals of the outer cortex are simple primary canals, whereas those of the deep cortex form small primary osteons (Fig. 2F). An avascular outer circumferential layer is absent. The bone matrix is isotropic (it appears red in online figure) under cross-polarized light with a lambda compensator in the transverse section (Fig. 2F) and anisotropic (blue in online figure) in the longitudinal section (Fig. 2H). This pattern suggests that bone matrix in the posterior region of the tibia is composed of parallel-fibered bone, with collagen fibers running parallel to the longitudinal axis of the tibia. Osteocyte lacunae have a rounded aspect in the transverse section (Fig. 2E,F) and an elongate spindle shape in the longitudinal section (Fig. 2G,H). The anterior and the lateral regions of the tibia are similar to the posterior region in all respects but one:

the lateral region contains a line of arrested growth split into two lines.

The stylopodial bones (femur and humerus) show a well-developed vascularization in the deep cortex, mainly formed by vascular canals parallel to the bone periphery (circular canals) connected through abundant radial anastomoses (Fig. 3A–D). This pattern of vascular orientation is more regular in the femur (Fig. 3A,B) than in the humerus (Fig. 3C,D), but vascular density decreases from the inner to the outer cortex in both cases. The bone matrix is made of either a scaffold of woven bone containing primary osteons (fibrolamellar bone; e.g., Fig. 3E,F) or a scaffold of parallel-fibered bone containing both simple vascular canals and primary osteons (e.g., Fig. 3G,H). We can observe the anisotropic (blue in online figure) aspect of the scaffold of bone matrix in a longitudinal section of the humerus under

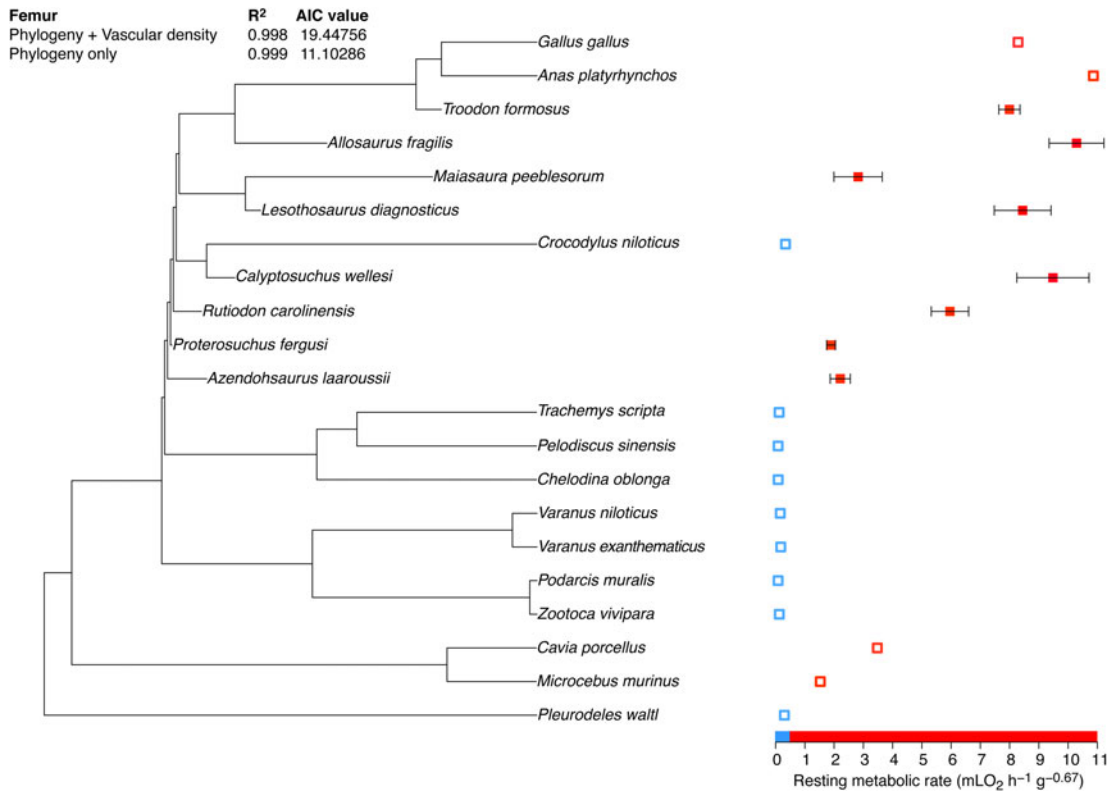


FIGURE 5. Resting metabolic rates quantified in a sample of extant tetrapods and inferred in a sample of extinct Archosaur-omopha using the phylogeny only. Data for *Azendohsaurus laaroussii* were obtained in this study and data for other taxa as well as the phylogeny were taken from Legendre et al. (2016). Resting metabolic rates inferred for *Azendohsaurus*, *Proterosuchus*, and *Maiasaura* are in the range of variation of extant mammals; values inferred for *Calyptosuchus*, *Lesothosaurus*, *Allosaurus*, and *Troodon* are in the range of variation of extant birds, whereas the value inferred for *Rutiodon* is intermediate.

polarized light, suggesting that it is made of parallel-fibered bone with collagen fibers oriented parallel to the main axis of the bone (Fig. 3H). Please note that the matrix around vascular canals appears isotropic (red in online figure) in this longitudinal section (Fig. 3H), whereas it appears anisotropic (blue in online figure) in the transverse section (Fig. 3G), suggesting that it is made of parallel-fibered bone forming primary osteons with collagen fibers perpendicular to the main axis of the humerus. Avascular outer circumferential layers or lines of arrested growth are absent in both femur and humerus (Fig. 3A–D).

In summary, vascular canals are more abundant in the deep cortex than in the outer cortex in all three bones, suggesting an ontogenetic decrease of bone growth rates (e.g., Fig. 2E). Considering that the avascular outer circumferential layer of parallel-fibered bone is absent

(we observed vascular canals near the bone periphery in many regions; e.g., Fig. 2E) and that lines of arrested growth are absent in all analyzed regions but one (the lateral region of the tibia), we conclude that the analyzed specimens were subadults. The two lines of arrested growth observed in the lateral region of the tibia probably correspond to the split of a single line formed during bone cortical drift, because they are absent in the anterior, posterior, and medial sides of the same section.

Inferring the Resting Metabolic Rate of *Azendohsaurus laaroussii*

First, we tested whether vascular density explains a significant fraction of the variation of resting metabolic rate using the sample of extant tetrapods published by Legendre et al. (2016). For this, we used phylogenetic generalized least-squares regressions (Grafen 1989). In

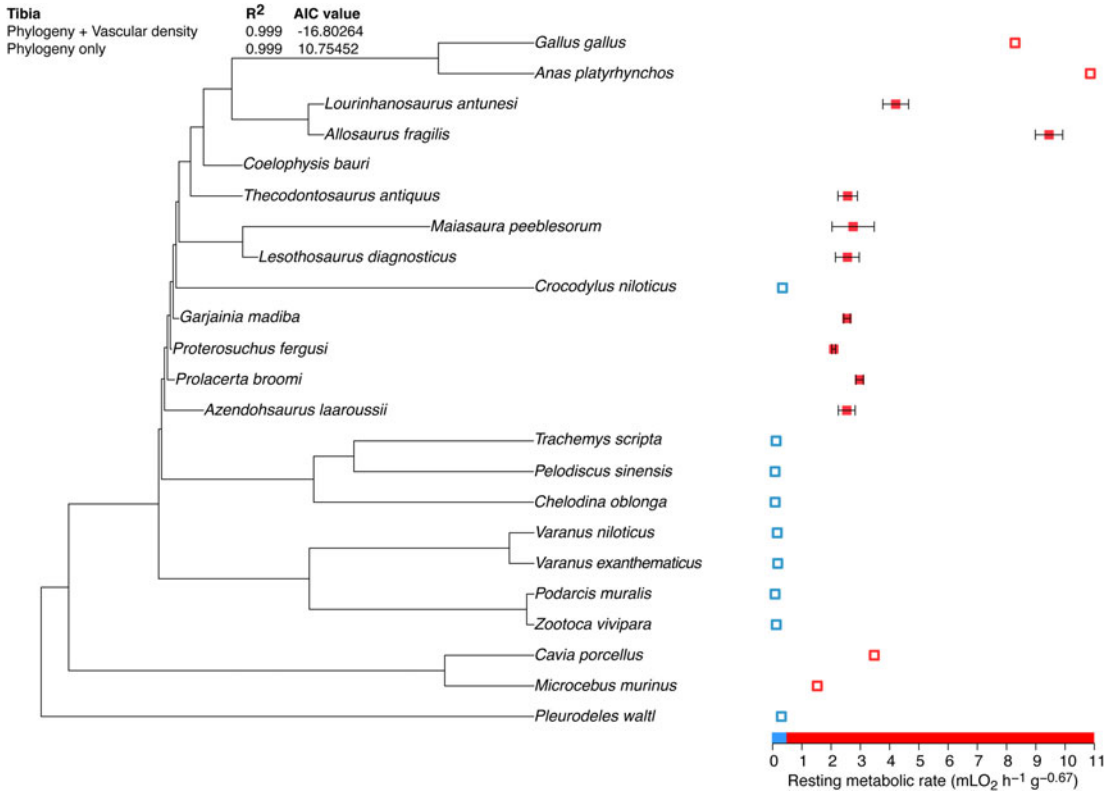


FIGURE 6. Resting metabolic rates quantified in a sample of extant tetrapods and inferred in a sample of extinct Archosauromorpha using the phylogeny and the vascular density of the tibia. Data for *Azendohsaurus laaroussii* were obtained in this study and data for other taxa as well as the phylogeny were taken from Legendre et al. (2016). Resting metabolic rate inferred for *Azendohsaurus*, *Prolacerta*, *Proterosuchus*, *Garjainia*, *Lesothosaurus*, *Maiasaura*, and *Thecodontosaurus* are in the range of variation of extant mammals; the value inferred for *Allosaurus* is in the range of variation of extant birds, whereas the value inferred for *Lourinhanosaurus* is intermediate.

all three cases (humerus, femur, and tibia), vascular density explained highly significant portions of the variation of resting metabolic rate (85%, 73.3%, and 78.9%, respectively). Thus, a priori we can confidently infer the resting metabolic rate of *A. laaroussii* using the vascular density values measured in the humerus, the femur, and the tibia (65.56, 34.83, and 47.19 vascular canals by square millimeter, respectively) and the comparative data published by Legendre et al. (2016).

Phylogenetic eigenvector maps (Guenard et al. 2013) includes an Akaike information criterion (AIC) procedure to select the explanatory variables (here, vascular density and/or the phylogeny) to be used to infer the response variable (here, the resting metabolic rate) of extinct taxa (here, *A. laaroussii* and the sample of extinct Archosauromorpha published by

Legendre et al. [2016]). According to the AIC procedure, the variable that maximizes the R^2 and minimizes the AIC value should be selected. In the case of the humerus, we obtained the same R^2 when using vascular density and the phylogeny and when using only the phylogeny, but the AIC value was lower when using both vascular density and the phylogeny (Fig. 4). We inferred a resting metabolic rate of $3.11 \text{ ml O}_2 \text{ h}^{-1} \text{ g}^{-0.67}$ and a confidence interval of $2.87\text{--}3.36 \text{ ml O}_2 \text{ h}^{-1} \text{ g}^{-0.67}$ for *A. laaroussii* using the phylogeny and vascular density of the humerus (Fig. 4). In the case of the femur, we found a slightly higher R^2 and a lower AIC value when using the phylogeny only (Fig. 5). We inferred a resting metabolic rate of $2.20 \text{ ml O}_2 \text{ h}^{-1} \text{ g}^{-0.67}$ and a confidence interval of $1.55\text{--}2.85 \text{ ml O}_2 \text{ h}^{-1} \text{ g}^{-0.67}$ for *A. laaroussii* using only the phylogeny

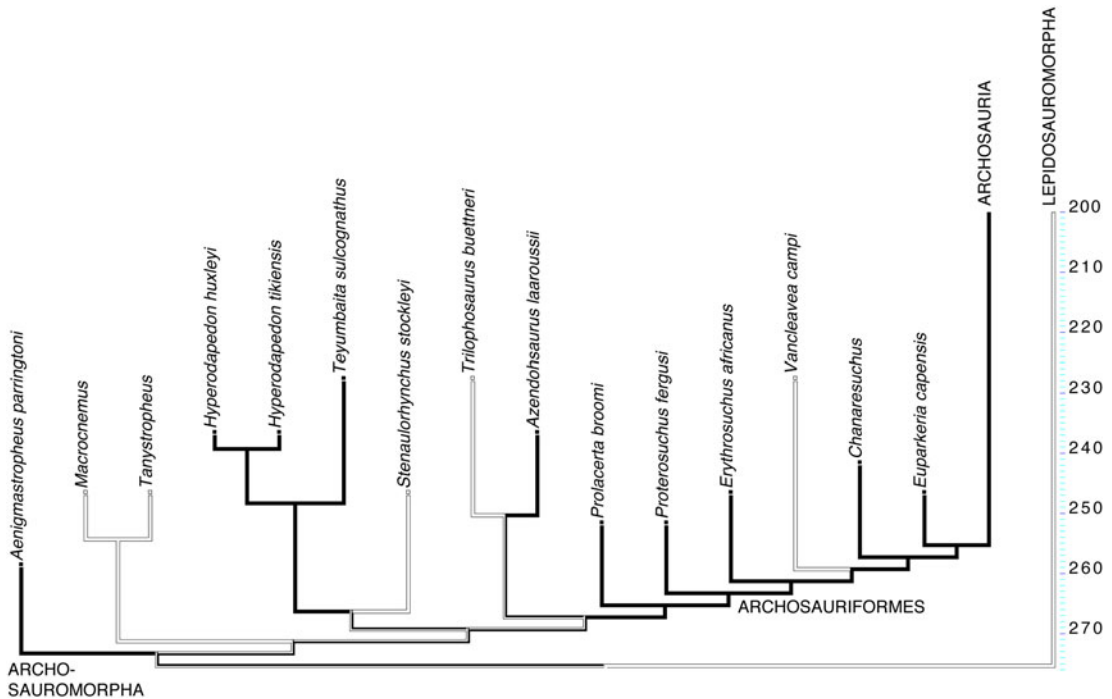


FIGURE 7. Optimization using parsimony of the presence of fibrolamellar bone in the stylopodial and zeugopodial bones of the Archosauromorpha analyzed to date (data summarized in Table 1). The topology is based on Nesbitt et al. (2009) for Archosauriformes and on Nesbitt et al. (2015) for non-archosauriform Archosauromorpha. The minimum ages of taxa are from the Paleobiology Database. Black branches indicate presence of fibrolamellar bone, white branches indicate absence, and black and white branches indicate uncertain character state.

(this is equivalent to an optimization; Fig. 5). Finally, in the case of the tibia, we obtained again the same R squared when using vascular density and the phylogeny and when using only the phylogeny, but the AIC value was lower when using both vascular density and the phylogeny (Fig. 6). We inferred a resting metabolic rate of $2.53 \text{ ml O}_2 \text{ h}^{-1} \text{ g}^{-0.67}$ and a confidence interval of $2.25\text{--}2.82 \text{ ml O}_2 \text{ h}^{-1} \text{ g}^{-0.67}$ for *A. laaroussii* using the phylogeny and the vascular density of the tibia (Fig. 6).

Discussion

Evolution of Fibrolamellar Bone in Archosauromorpha

The formation of fibrolamellar bone is very energy consuming, because it involves the combined action of static osteogenesis (to form a scaffold of woven bone at high growth rates involving high rates of protein synthesis) and dynamic osteogenesis (osteonal infilling with

lamellar or nonlamellar parallel-fibered bone) (Prondvai et al. 2014). Therefore the capacity for reaching and maintaining very high bone growth rates during ontogeny, recorded by the presence of fibrolamellar bone in the bone cortex, may be a reliable proxy to infer the metabolic rate of extinct animals (see “Introduction”). Four previous studies have analyzed the evolution of the presence of fibrolamellar bone in Archosauromorpha in a phylogenetic context (Botha-Brink and Smith 2011; Mukherjee 2015; Veiga et al. 2015; Jaquier and Scheyer 2017). Here, we performed parsimony optimizations of this character state (Fig. 7, Supplementary Figs. 2, 3) using our observations on the bone histology of *A. laaroussii* and previously published observations on other Archosauromorpha (summarized in Table 1).

We observed three bone tissue types in the humerus, femur, and tibia of *A. laaroussii*: (1) avascular lamellar zonal bone (e.g., Fig. 2A–D); (2) a cortex formed by a scaffold of parallel-fibered bone (with collagen fibers

TABLE 1. Bibliographic compilation of the presence/absence of fibrolamellar complex in the long bones of the non-archosaurian Archosauromorpha analyzed to date.

Taxa	Presence of fibrolamellar complex	Skeletal elements	References	Figures within references
<i>Aenigmastropheus parringtoni</i>	1	Humerus (?)	Ezcurra et al. (2014)	Fig. 15A–D
<i>Azendohsaurus laaroussii</i>	1	Humerus, femur	Cubo and Jalil, this study	Fig. 2E,F
<i>Chanaresuchus</i>	1	“Long bone”	Ricqlès et al. (2008)	Plate 2, Fig. 3
<i>Erythrosuchus africanus</i>	1	Fibula	Ricqlès et al. (2008)	Plate 1, Fig. 4
<i>Erythrosuchus africanus</i>	1	Radius, tibia	Botha-Brink and Smith (2011)	Fig. 4A,B
<i>Euparkeria capensis</i>	0	Humerus or femur	Ricqlès et al. (2008)	Plate 2, Fig. 4
<i>Euparkeria capensis</i>	0	Humerus, femur, tibia, fibula	Botha-Brink and Smith (2011)	Figs. 5A–D and 6A, B
<i>Euparkeria capensis</i>	1	Humerus	Legendre et al. (2013)	Fig. 1A,B
<i>Hyperodapedon huxleyi</i>	1	Humerus, radius, femur, tibia	Mukherjee (2015)	Figs. 2–7
<i>Hyperodapedon tikiensis</i>	1	Humerus, radius, femur, tibia	Mukherjee (2015)	Figs. 2–7
<i>Macrocnemus bassanii</i>	0		Jaquier and Scheyer (2017)	
<i>Prolacerta broomi</i>	1	Tibia	Botha-Brink and Smith (2011)	Fig. 2A–C
<i>Proterosuchus fergusi</i>	1	Femur, tibia, fibula	Botha-Brink and Smith (2011)	Fig. 3A–D
<i>Stenaulorhynchus stockleyi</i>	0	Femur, tibia	Werning and Nesbitt (2016)	Figs. 3, 4
<i>Tanystropheus</i>	0	Humerus, femur	Jaquier and Scheyer (2017)	Fig. 2A,B
<i>Teyumbaita sulcognathus</i>	1	Tibia	Veiga et al. (2015)	Fig. 1B
<i>Trilophosaurus buettneri</i>	0	Humerus, ulna	Werning and Irmis (2011)	
<i>Vancleavea campi</i>	0	Humerus	Nesbitt et al. (2009)	Fig. 21B

parallel to the longitudinal axis of the bone) containing either small primary osteons infilled by lamellar parallel-fibered bone (inner part of the cortex; Fig. 2F) or simple vascular canals (outer part of the cortex; Fig. 2F), and (3) fibrolamellar bone (e.g., Fig. 3E,F). Therefore, we coded the presence of FLB for *Azendohsaurus* (Fig. 7, Supplementary Figs. 2, 3).

We coded the presence of FLB for Archosauria, because this character state has been reported both in Pseudosuchia (e.g., Ricqlès et al. 2003; Padian et al. 2004; Nesbitt 2007; Tumarkin-Deratzian 2007) and in Ornithodira (Ricqlès et al. 2000; Padian et al. 2004; Cubo et al. 2015). Consistently, Cubo et al. (2012) inferred a high bone growth rate for the last common ancestor of archosaurs. Lepidosauromorpha has been chosen as an outgroup and is characterized by the absence of this character state (Fig. 7, Supplementary Figs. 2, 3).

We performed an optimization of the presence of FLB onto the phylogeny of Archosauromorpha published by Nesbitt et al. (2015) (Fig. 7). Moreover, we carried out two supplementary optimizations of the presence of FLB using the phylogenies of Archosauromorpha published by Pritchard et al. (2015) (Supplementary Fig. 2) and Ezcurra (2016)

(Supplementary Fig. 3). All three analyses showed a flickering on-and-off pattern that prevents inferring the primitive condition for this clade. Moreover, the parsimony method fails to find the condition for the four more inclusive (basal) nodes of the clade. The only robust conclusion obtained in the three analyses is congruent with that published by Botha-Brink and Smith (2011): the fibrolamellar bone was acquired by the last common ancestor of *Prolacerta*–archosauriforms, with a reversion in *Vancleavea* (Fig. 7, Supplementary Figs. 2, 3).

Constraining the Phylogenetic Frame of the Acquisition of Endothermy by Archosauromorpha

The resting metabolic rate may be a good proxy to infer the thermometabolic regime (endothermy vs. ectothermy) of extinct organisms, because thermogenesis is very energy consuming (see “Introduction”). Legendre et al. (2016) used this proxy in Archosauromorpha and concluded that endothermy may have been acquired by the last common ancestor of the clade *Prolacerta*–archosauriforms. We inferred the resting metabolic rate of a member of the sister group of this clade (*Azendohsaurus laaroussii*: Allokokotosauria) as the next step to

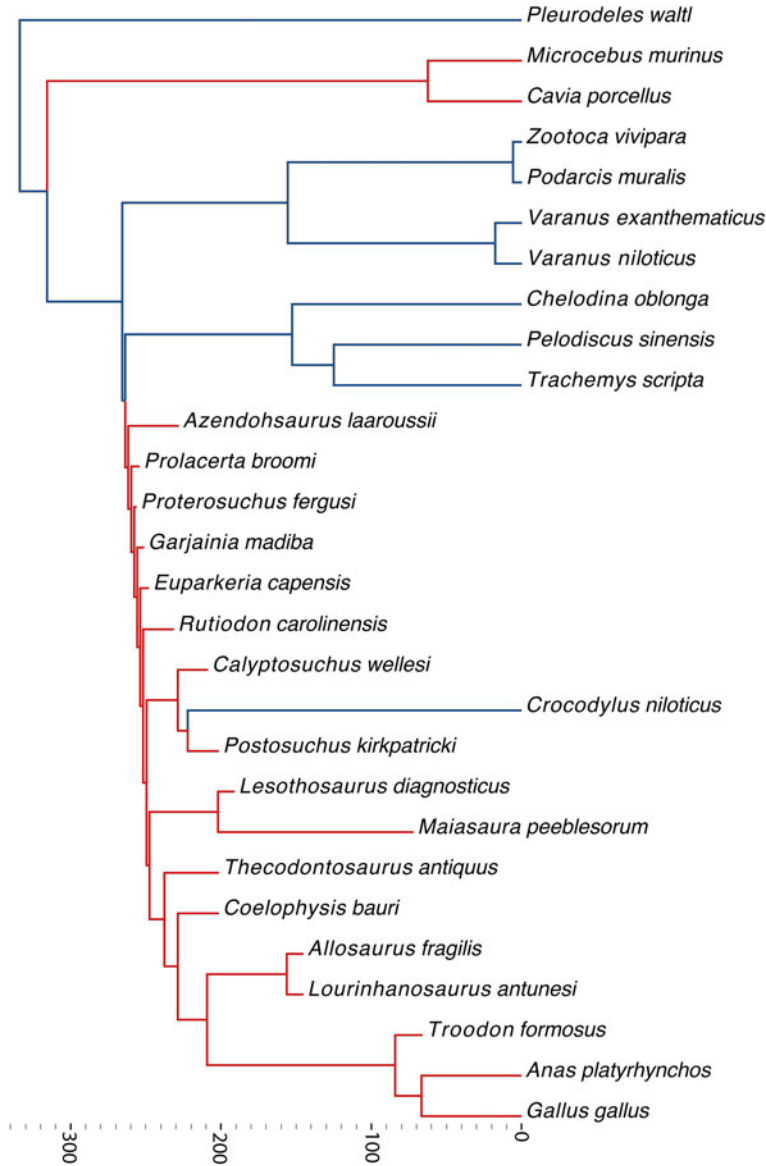


FIGURE 8. Optimization using parsimony of the presence of endothermy in a sample of tetrapods. The presence of endothermy was inferred in extinct tetrapods using resting metabolic rates estimated through phylogenetic eigenvector maps. Dark gray (red online) corresponds to the presence of endothermy and light gray (blue online) to the presence of ectothermy. The phylogeny has been taken from Legendre et al. (2016).

better constrain the phylogenetic frame of the acquisition of endothermy by Archosauromorpha. Moreover, we inferred resting metabolic rate values for the sample of 14 extinct Archosauromorpha analyzed by Legendre et al. (2016). The values inferred for all these taxa are included in the range of variation measured in the sample of extant endotherms (mammals and birds) (Figs. 4–6). Considering that

thermogenesis is very energy consuming, we can reasonably assume that all these taxa were endotherms. A parsimony optimization of the presence of endothermy in the whole sample (including extant taxa of known thermometabolism and extinct taxa of inferred thermometabolism) shows that endothermy was acquired twice, by mammals and by the last common ancestor of the clade

Azendohsaurus–archosauriforms, and that within this last clade there is a reversion in Crocodylia (Fig. 8). Considering that many archosauriforms have been found in the Permian and that endothermy may have been acquired in a more inclusive clade (*Azendohsaurus*–archosauriforms), this key evolutionary event probably took place in the Permian. Bernard et al. (2010) inferred fully developed endothermy for ichthyosaurs and plesiosaurs and incipient endothermy for mosasaurs using a geochemical approach. These conclusions are congruent with those obtained using a paleohistological approach (Buffrénil and Mazin [1990] for ichthyosaurs; Fleischle et al. [2018] for plesiosaurs; and Houssaye et al. [2013] for mosasaurs). Thermogenetic mechanisms have also been described in Actinopterygii: at the extraocular muscles that warm the eyes and brain in billfishes (Xiphiidae) and in the butterfly kingfish *Gasterochisma melampus* (Scombridae: Gasterochismatinae) (Davesne et al. 2018). Future research on the biochemical basis of thermogenesis in extant taxa and on paleobiological inference of resting metabolic rates in extinct taxa are needed to elucidate the origin and the evolutionary patterns of endothermy in Osteichthyes.

Acknowledgments

We thank R. Allain, curator of paleontology at the MNHN, for giving us permission to perform histological analyses in the right humerus MNHN.F ALM 435, the left femur MNHN.F ALM 497, and the right tibia MNHN.F ALM 369 of *A. laaroussii*. We also thank D. Germain, curator of the vertebrate hard tissues histological collection of the MNHN, for including the thin sections produced in this study in that collection. Thanks also to H. Lamrous for the preparation of the thin sections, to P. Loubry for the photos, and to S. Fernandez for the drawings. Finally, we thank H. Woodward and an anonymous reviewer for their constructive comments.

Literature Cited

Bernard, A., C. Lécuyer, P. Vincent, R. Amiot, N. Bardet, N., E. Buffetaut, G. Cuny, F. Fourel, F. Martineau, J. M. Mazin, and A. Prieur. 2010. Regulation of body temperature by some Mesozoic marine reptiles. *Science* 328:1379–1382.

- Bonaparte, J. F. 1976. *Pisanosaurus mertii* Casamiquela and the origin of the Ornithischia. *Journal of Paleontology* 50:808–820.
- Botha-Brink, J., and R. M. H. Smith. 2011. Osteohistology of the Triassic Archosauromorphs *Prolacerta*, *Proterosuchus*, *Euparkeria*, and *Erythrosuchus* from the Karoo Basin of South Africa. *Journal of Vertebrate Paleontology* 31:1238–1254.
- Buffrénil, V. de, and J. M. Mazin 1990. Bone histology of the ichthyosaurs: comparative data and functional interpretation. *Paleobiology* 16:435–447.
- Cubo, J., N. Le Roy, C. Martínez-Maza, and L. Montes. 2012. Paleohistological estimation of bone growth rate in extinct archosaurs. *Paleobiology* 38:335–349.
- Cubo, J., H. Woodward, E. Wolff, and J. R. Horner. 2015. First reported cases of biomechanically adaptive bone modeling in non-avian dinosaurs. *PLoS ONE* 10:e0131131.
- Cubo, J., M. Hui, F. Clarac, and A. Quilhac. 2017. Static osteogenesis does not precede dynamic osteogenesis in periosteal ossification of *Pleurodeles* (Caudata, Amphibia) and *Pogona* (Squamata, Lepidosauria). *Journal of Morphology* 278:621–628.
- Davesne, D., F. J. Meunier, M. Friedman, R. B. J. Benson, and O. Otero 2018. Histology of the endothermic opah (*Lampris* sp.) suggests a new structure–function relationship in teleost fish bone. *Biology Letters* 14:20180270. doi: 10.1098/rsbl.2018.0270.
- Dutuit, J.-M. 1972. Découverte d'un Dinosaurien ornithischien dans le Trias supérieur de l'Atlas occidental marocain. *Comptes Rendus de l'Académie des Sciences, Paris* 275:2841–2844.
- . 1976. Introduction à l'étude paléontologique du Trias continental marocain. Description des premiers Stégocéphales recueillis dans le Couloir d'Argana (Atlas occidental). *Mémoires du Muséum National d'Histoire Naturelle, nouvelle série C* 36:1–253.
- Ezcurra, M. D. 2016. The phylogenetic relationships of basal archosauromorphs, with an emphasis on the systematics of proterosuchian archosauriforms. *PeerJ* 4:e1778.
- Ezcurra, M. D., T. M. Scheyer, and R. J. Butler. 2014. The origin and early evolution of Sauria: Reassessing the Permian saurian fossil record and the timing of the crocodile-lizard divergence. *PLoS ONE* 9:e89165.
- Ferretti, A., C. Palumbo, M. Contri, and G. Marotti. 2002. Static and dynamic osteogenesis: two different types of bone formation. *Anatomy and Embryology* 206:21–29.
- Fleischle, C. V., T. Wintrich, and P. M. Sander 2018. Quantitative histological models suggest endothermy in plesiosaurs. *PeerJ* 6:25. doi: 10.7717/peerj.4955.
- Flynn, J. J., J. M. Parrish, B. Rakotosamimanana, W. F. Simpson, R. B. Whitley, and A. R. Wyss. 1999. A Triassic fauna from Madagascar, including early dinosaurs. *Science* 286:763–765.
- Flynn, J. J., S. J. Nesbitt, J. M. Parrish, R. Ranivoharimana, and A. R. Wyss. 2010. A new species of *Azendohsaurus* (Diapsida: Archosauromorpha) from the Triassic Isalo Group of southeastern Madagascar: cranium and mandible. *Palaeontology* 53:669–688.
- Francillon-Vieillot, H., V. de Buffrénil, J. Castanet, J. Geraudie, F. Meunier, J. Y. Sire, L. Zylberberg, and A. de Ricqlès. 1990. Microstructure and mineralization of vertebrate skeletal tissues. Pp. 471–548 in J. G. Carter, ed. *Skeletal biomineralization: patterns, processes and evolutionary trends*. Van Nostrand Reinhold, New York.
- Galton, P. M. 1985. Diet of Prosauropod dinosaurs from the Late Triassic and Early Jurassic. *Lethaia* 18:105–123.
- . 1990. Basal Sauropodomorpha—Prosauropoda. Pp. 320–344 in D. B. Weishampel, P. Dodson, and H. Osmólska, eds. *The Dinosauria*. University of California Press, Berkeley.
- Gauffre, F.-X. 1993. The prosauropod dinosaur *Azendohsaurus laaroussii* from the Upper Triassic of Morocco. *Palaeontology* 36:897–908.
- Grafen, A. 1989. The phylogenetic regression. *Philosophical Transactions of the Royal Society of London B* 326:119–157.
- Guenard, G., P. Legendre, and P. Peres-Neto. 2013. Phylogenetic eigenvector maps: a framework to model and predict species traits. *Methods in Ecology and Evolution* 4:1120–1131.

- Houssaye, A., J. Lindgren, R. Pellegrini, A. H. Lee, D. Germain, and M. J. Polcyn. 2013. Microanatomical and histological features in the long bones of mosasaurine mosasaurs (Reptilia, Squamata) —implications for aquatic adaptation and growth rates. *PLoS ONE* 8(10):1–12. doi:10.1371/journal.pone.0076741.
- Hunt, A. P., and S. P. Lucas. 1994. Ornithischian dinosaurs from the Upper Triassic of the United States. Pp. 227–241 in N. C. Fraser and H.-D. Sues, eds. *In the shadow of the dinosaurs. Early Mesozoic tetrapods*. Cambridge University Press, Cambridge.
- Jalil, N. E., and F. Knoll. 2002. Is *Azendohsaurus laaroussii* (Carnian Morocco) a dinosaur? *Journal of Vertebrate Paleontology* 22 (Suppl. to No. 3):70A.
- Jaquier, V. P., and T. M. Scheyer. 2017. Bone histology of the Middle Triassic long-necked reptiles *Tanystropheus* and *Macrocnemus* (Archosauromorpha, Protosauria). *Journal of Vertebrate Paleontology* 37:e1296456.
- Khalidoun, F. 2014. Les vertébrés du Permien et du Trias du Maroc (Bassin d'Argana, Haut Atlas Occidental) avec la réévaluation d'*Azendohsaurus laaroussii* (Reptilia, Archosauromorpha) et la description de Reptilia Moradisaurinae et Rhynchosauria nouveaux: anatomie, relations phylogénétiques et implications biostatigraphiques. Unpublished Ph.D. thesis. University Cadi Ayyad, Marrakesh, Morocco. 342 pp.
- Lamm, E. T. 2013. Preparation and sectioning of specimens. Pp. 55–160 in *Bone histology of fossil tetrapods: advancing methods, analysis, and interpretation*. University of California Press, Berkeley.
- Legendre, L. J., L. Segalen, and J. Cubo. 2013. Evidence for high bone growth rate in *Euparkeria* obtained using a new paleohistological inference model for the humerus. *Journal of Vertebrate Paleontology* 33:1343–1350.
- Legendre, L. J., G. Guenard, J. Botha-Brink, and J. Cubo. 2016. Palaeohistological evidence for ancestral high metabolic rate in Archosaurs. *Systematic Biology* 65:989–996.
- Lowell, B. B., and B. M. Spiegelman. 2000. Towards a molecular understanding of adaptive thermogenesis. *Nature* 404:652–660.
- Maddison, W. P., and D. R. Maddison. 2015. Mesquite: a modular system for evolutionary analysis. <http://www.mesquiteproject.org>.
- Marotti, G. 2010. Static and dynamic osteogenesis. *Italian Journal of Anatomy and Embryology/Archivio italiano di anatomia ed embriologia* 115:123–126.
- Montes, L., N. Le Roy, M. Perret, V. De Buffrenil, J. Castanet, and J. Cubo. 2007. Relationships between bone growth rate, body mass and resting metabolic rate in growing amniotes: a phylogenetic approach. *Biological Journal of the Linnean Society* 92:63–76.
- Mukherjee, D. 2015. New insights from bone microanatomy of the Late Triassic *Hyperodapedon* (Archosauromorpha, Rhynchosauria): implications for archosauromorph growth strategy. *Palaeontology* 58:313–339.
- Nesbitt, S. 2007. The anatomy of *Effigia okeeffeae* (Archosauria, Suchia), theropod-like convergence, and the distribution of related taxa. *Bulletin of the American Museum of Natural History* 302:1–84.
- Nesbitt, S. J., M. R. Stocker, B. J. Small, and A. Downs. 2009. The osteology and relationships of *Vancleavea campi* (Reptilia: Archosauriformes). *Zoological Journal of the Linnean Society* 157:814–864.
- Nesbitt, S. J., J. J. Flynn, A. C. Pritchard, J. M. Parrish, L. Ranivoharimanana, and A. R. Wyss. 2015. Postcranial osteology of *Azendohsaurus madagaskarensis* (?middle to Upper Triassic, Isalo Group, Madagascar) and its systematic position among stem archosaur reptiles. *Bulletin of the American Museum of Natural History* 398:1–126.
- Nowack, J., S. Giroud, W. Arnold, and T. Ruf. 2017. Muscle non-shivering thermogenesis and its role in the evolution of endothermy. *Frontiers in Physiology* 8:ar889.
- Orme, D., R. Freckleton, G. Thomas, T. Petzoldt, S. Fritz, N. Isaac, and W. Pearse. 2013. Caper: comparative analyses of phylogenetics and evolution in R. <https://CRAN.R-project.org/package=caper>.
- Padian, K., and J. R. Horner. 2002. Typology versus transformation in the origin of birds. *Trends in Ecology and Evolution* 17:120–124.
- Padian, K., J. R. Horner, and A. De Ricqlès. 2004. Growth in small dinosaurs and pterosaurs: the evolution of archosaurian growth strategies. *Journal of Vertebrate Paleontology* 24:555–571.
- Palumbo, C., M. Ferretti, and G. Marotti. 2004. Osteocyte dendrogenesis in static and dynamic bone formation: an ultrastructural study. *Anatomical Record A* 278A:474–480.
- Pritchard, A. C., A. H. Turner, S. J. Nesbitt, R. B. Irmis, and N. D. Smith. 2015. Late Triassic tanystropheids (Reptilia, Archosauromorpha) from northern New Mexico (Petrified Forest Member, Chinle Formation) and the biogeography, functional morphology, and evolution of Tanystropheidae. *Journal of Vertebrate Paleontology* 35:e911186.
- Prondvai, E., K. H. W. Stein, A. de Ricqlès, and J. Cubo. 2014. Development-based revision of bone tissue classification: the importance of semantics for science. *Biological Journal of the Linnean Society* 112:799–816.
- R Core Team. 2016. R: a language and environment for statistical computing. R Foundation for Statistical Computing, Vienna, Austria. <http://www.R-project.org>.
- Ricqlès, A. de, K. Padian, J. R. Horner, and H. Francillon-Vieillot. 2000. Palaeohistology of the bones of pterosaurs (Reptilia: Archosauria): anatomy, ontogeny, and biomechanical implications. *Zoological Journal of the Linnean Society* 129:349–385.
- Ricqlès, A. de, K. Padian, and J. R. Horner. 2003. On the bone histology of some Triassic pseudosuchian archosaurs and related taxa. *Annales de Paléontologie* 89:67–101.
- Ricqlès, A. de, K. Padian, F. Knoll, and J. R. Horner. 2008. On the origin of high growth rates in archosaurs and their ancient relatives: complementary histological studies on Triassic archosauriforms and the problem of a “phylogenetic signal” in bone histology. *Annales de Paléontologie* 94:57–76.
- Rowland, L. A., N. C. Bal, and M. Periasamy. 2015. The role of skeletal-muscle-based thermogenic mechanisms in vertebrate endothermy. *Biological Reviews* 90:1279–1297.
- Stein, K., and E. Prondvai. 2014. Rethinking the nature of fibrolamellar bone: an integrative biological revision of sauropod plexiform bone formation. *Biological Reviews* 89:24–47.
- Thulborn, R. A. 1973. Teeth of ornithischian dinosaurs from the Upper Jurassic of Portugal. *Serviços Geológicos de Portugal, Memoria* 22: 89–134.
- . 1974. A new heterodontosaurid dinosaur (Reptilia: Ornithischia) from the Upper Triassic Red Beds of Lesotho. *Zoological Journal of the Linnean Society of London* 55:151–175.
- Tumarkin-Deratzian, A. R. 2007. Fibrolamellar bone in wild adult *Alligator mississippiensis*. *Journal of Herpetology* 41:341–345.
- Veiga, F. H., M. B. Soares, and J. M. Sayao. 2015. Osteohistology of hyperodapedontine rhynchosaurs from the Upper Triassic of Southern Brazil. *Acta Palaeontologica Polonica* 60:829–836.
- Weishampel, D. B. 1990. Dinosaurian distribution. Pp. 63–139 in D. B. Weishampel, P. Dodson, and H. Osmólska, eds. *The Dinosauria*. University of California Press, Berkeley.
- Werning, S., and R. B. Irmis. 2011. Reconstructing growth of the basal archosauromorph *Trilophosaurus*. *Integrative and Comparative Biology* 51:E147.
- Werning, S., and S. J. Nesbitt. 2016. Bone histology and growth in *Stenaulorhynchus stockleyi* (Archosauromorpha: Rhynchosauria) from the Middle Triassic of the Ruhuhu Basin of Tanzania. *Comptes Rendus Palevol* 15:163–175.